

On the design of multi-site microelectrodes for neuronal recordings

Ulrich G. Hofmann*, Med. Universität zu Lübeck, Institut für Signalverarbeitung und Prozeßrechentechnik, Seelandstr. 1a), 23569 Lübeck, Germany.

Erik De Schutter, Universitaire Instelling Antwerpen, Laboratory for Theoretical Neurobiology, 2610 Antwerp, Belgium

Ken Yoshida, Aalborg Universitet, Center for Sensory-Motor Interaction, 9220 Aalborg, Denmark

Marco de Curtis, Istituto Nazionale Neurologico Carlo Besta, Neurofisiologia Sperimentale, 20133 Milano, Italy

Uwe Thomas, Uwe Thomas RECORDING, 35394 Giessen, Germany

Peter Norlin, ACREO AB, 16440 Stockholm-Kista, Sweden

*To whom correspondence should be addressed: hofmann@isip.mu-luebeck.de; fax: +49.451.3909.555; phone: +49.451.3909.552

Abstract

The current understanding of how the nervous system functions is based on numerous observations of the behavior of single neuronal units or a small ensemble of units correlated to some external stimulation or behavioral event. However, the processing power of the nervous system lies in its network and interconnections. Thus the key to understanding the nervous system is to make simultaneous observations of the activity of numerous cells from within a functioning brain.

The objective of the EU funded project VSAMUEL is to develop such a system based on silicon microelectrode arrays for acquiring signals from nervous tissue *in vivo*. The system will utilize advanced micro-structuring based on SOI wafers to design and fabricate probes with up to 128 recording sites: microelectrodes placed on tiny fork shaped probes. Those probes and the location of their shafts and recording sites, the probe design for short, does not only have to obey the rules imposed on them by the utilized micro-machining techniques, but by anatomical requirements as well, as demanded by the neurobiological experiment. The whole project not only includes the development of easy-to-use connectors and suitable multi-channel signal amplifiers, but also a novel high-quality, high-throughput data acquisition system (DAQ), based on commonly available PC-computers and signal processing boards in conjunction with novel signal processing software.

1 The project VSAMUEL

1.1 Introduction

Modern neuroscience and our understanding of how the brain and its neural units work, is undisputably connected to the experimental ability of detecting their natural means of communication by electrical activity [1,2]. Even though extracellular recording from single cells is performed routinely, little is still known about network- and higher level activity. Intercepting this level of information processing requires the technological ability to place a multiplicity of recording sites in close proximity to cells in question or precisely probing the neuronal function over and over again [3-5]. The use of standard microelectrodes

or even tetrodes not only requires extremely difficult surgical procedures, but also traumatizes the penetrated tissue, due to the number of probes with rods of diameters of up to several tens of microns. [6-8].

It seems therefore highly desirable, to insert with *one* single penetration and only a *few* thin rods as many recording sites as possible into the area of interest (see **fig.1**). This may be performed by micromachined, batch-fabricated and inexpensive silicon forks, carrying tens of micrometer-sized recording sites, as already proposed earlier [9]. The basic development of this technological goal was already achieved in the 80's [10,11], and valuable data was taken later [12-14], but real widespread use in neuroscience research has not truly been achieved yet. We attribute this, besides the delicate handling of silicon multisite microelectrodes,

in part, to a lack of appropriate, easy to use and inexpensive data acquisition systems, which relieves the researcher from troublesome technological issues.

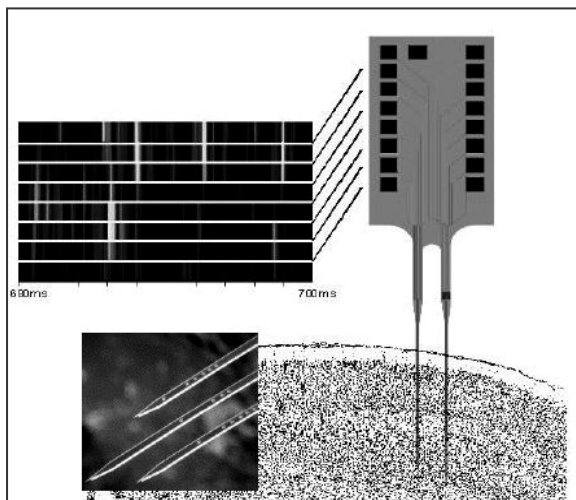


Figure 1 Schematic sketch of a fork-shaped, two-prong multisite microelectrode probe of an earlier design [15] inserted into a rats cortex. The lower insert displays recording sites on the shaft's sides; the upper insert illustrates a brief period of 8-channel recording, gray-scale coded for amplitude and arranged following their vertical arrangement [16].

1.2. VSAMUEL overview

We therefore aim with our project VSAMUEL towards the development of easy-to-use batch-fabricated multisite microelectrodes (see **fig.2 #2**) in conjunction with a similarly easy-to-use recording system, based on inexpensive digital signal processing computer hardware (fig.2 #1), custom built multichannel amplifiers (fig.2 #3) and adaptable recording software. The completed system has to prove its general usability by testing it under the rigid conditions of physiological experiments: both, *in vitro* in a whole cell preparation (fig.2 #5), as well as *in vivo* with central and peripheral nervous structures (fig.2 #4,6,7).

1.3 Hardware description

At the time of the writing of this text most of this system (aside from the microprobes) is still under development. However, several sections have been implemented: The data acquisition system is based on Texas Instruments most recent floating point DSP chip, the TMS320C670x on a PCI-board by Innovative Integration (Thousand Oaks, CA) called M67. Each M67 has 2 data processing pipelines, which are multiplexed to 4 A/D converters each, which in term are multiplexed to 4 differential input channel, adding up to 32 channels on a single board.

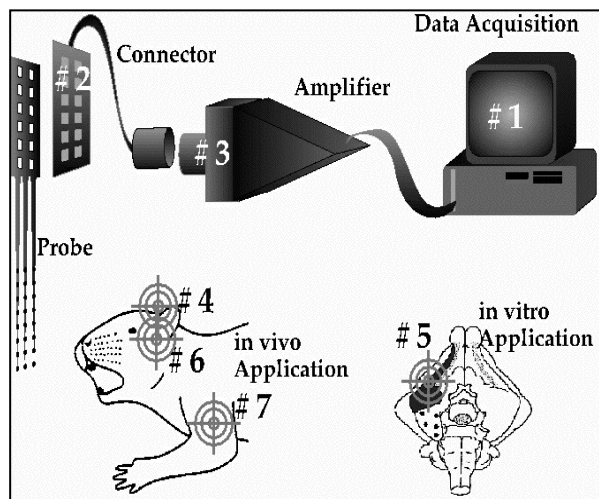


Figure 2 Schematic overview over the whole project VSAMUEL: #1 represents the data acquisition hard- and software, based on off-the-shelf digital signal processing boards, #2 displays the important, combined developed microprobes and their interconnects to the #3 pre-amplifier/amplifier system.

M67 cards are stackable to larger systems and will therefore lead to 128 acquisition channels in VSAMUEL's final stage. The custom made DSP-control software runs (as do the M67 cards) on a personal computer under Windows NT in a server mode. User command inputs to the computer are communicated using TCP/IP locally, and in future even remotely.

The incoming data stream is digitized with 50 kSamples/sec, but compressed by a wavelet scheme following the quality requirements of the user (low compression - high detail content - low recording capacity for permanent storage; less detail - longer recording sessions) [17].

The amplifier rack is a new design by Uwe Thomas RECORDING (Giessen, FRG) and amplifies the channels either manually or PC-serial port controlled with factors up to 10000. Low-noise pre-amplifier banks for 32 channels are used for impedance adjustment as well as increasing the original signal by a factor of 20.

The electrical connection to our silicon probes is made by a ZIF-connector on the pre-amp side and a several cm long, flexible PC-board at the probe (see **fig.3 #6**). The probe (fig.3 #1) in our prototype setup is wire-bonded (fig.3 #2) to the flex-board (fig.3 #4) on a rigid fixture (fig.3 #5) accessible to standard micromanipulators. The probe is held firmly and precisely controlled in place on its fixture, first by a mechanical lead groove and second by an epoxy drop. The latter is supposed to seal the delicate connections to the aggressive environment *in situ*.

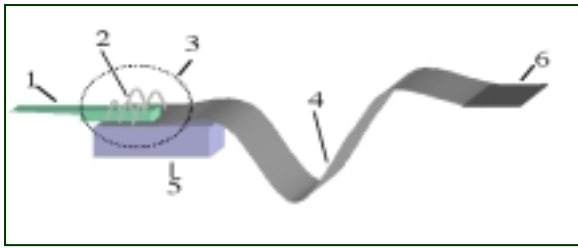


Figure 3 Schematic drawing of a probe (1) wire bonded (2) to a flexible PC-board (4) on a carrier (5). The bonded probe is epoxy sealed (3) and may be connected via the stiffened flex-board (6) to a zero-insertion-force connector on the pre-amp.

2 Silicon probes

2.1 General considerations

The most general consideration, one has to take into account for designing silicon based, multi-prong, multisite microelectrodes, is their duration of deployment within the brain in question. In other words, is the experiment under consideration an acute experiment, where the recordings have to be made the same session as the insertion takes place? Or do we intend to perform a longer-term survival experiment. The latter allows for at least partial recovery of the tissue penetrated by the probe, but needs for obvious reasons quite sturdy mechanical and interconnecting features [6, 18, 19]. Another advantage, besides more recordings possible with less time-consuming surgical efforts, is the option to ignore widespread dimpling effects of brain, which not only affect the areas close to the penetrating structure, but distant areas as well [20]. The recovery period seems to reestablish broken connections and networks [6].

Acute experiments, on the other hand, rely on recordings right after insertion, which means that the tissue damage by either factors - penetration and dimpling - has to be minimized. Ideally, the prongs would be infinitesimally small, minimally displacing the tissue and, therefore, minimally disrupting the interconnections. Unfortunately, the prongs must be of a reasonable size to carry electrode sites as well as provide a minimum amount of mechanical stability. In fact, silicon probes with widths between 15 μm and 40 μm , and thicknesses between 15 μm and 25 μm have been fabricated [21-23]. By comparison, single site microwires typically have diameters of about 50 μm . [6, 24]. Thinner prongs are not advisable, since they have to penetrate on insertion at least through the tough pial membrane. This requires a loading force of up to 2mN per prong and may therefore lead to uncontrolled buckling of a thin prong [20, 25, 26].

The minimal achievable width of a single prong is given by the size and number of recording sites and the space of connecting traces. Its minimal length is given by the deployment depth of recording sites under the brain surface (see **fig.4**), but may not exceed the length calculated by Euler-buckling [25].

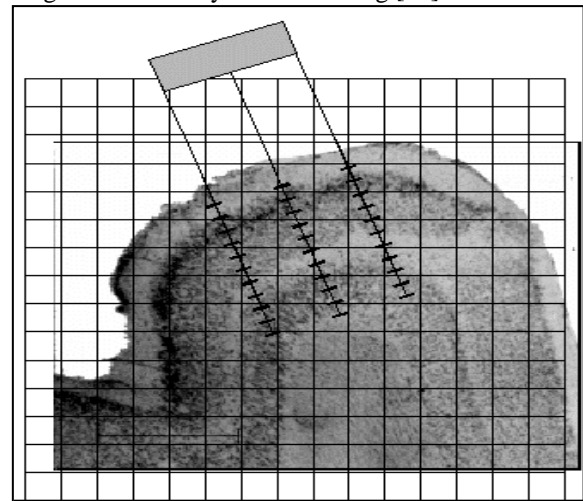


Figure 4 Coronal slice of a guinea pig's enthorhinal cortex with a stereotaxic 250 μm grid overlaid. Positions of interest, intended for probe deployment are marked on a three prong probe schematic.

Another aspect, fostering easy insertion, considers the shape of the very tip of silicon probes: Edell [27] proposed the superiority of a pencil-like and pointy tip over one with a line-type or even plane-like tip. This was in part empirically verified, but due to the mechanical features of the pial membrane, the taper and the sidewall structure of the prong's working end may be of importance as well [20]. We, therefore, favor prongs which have very sleek side walls and small taper angles (4° taper), which may be fabricated using Deep Reactive Ion Etching (DRIE, [28]). The high aspect ratio achievable by this process leads on the other hand to a line-shaped tip structure, which may for future experiments be improved by beveling it down to a pencil-shaped structure [27].

One final design aspect relates to the handling of single probes: It is our desire to allow the end user, who may or may not be experienced with fragile silicon structures, to handle even single probes on his own. Each probes base plate, which includes bond pads consistent with standard ultrasonic bonding, keeps for that reason full wafer thickness. This enables their handling by general use tools, like surgical tweezers.

2.2 Process overview

In order to achieve a consistent probe thickness of 25 μm over the whole production wafer, our process

starts from a "Silicon on Insulator" (SOI) wafer, with an oxide layer 25µm under the surface. This enables us later during the process to keep the whole wafer as long as possible intact. The process (see **fig.5 A**) itself utilizes optimized low-stress insulator and metal deposition, to avoid bending of the long and narrow prongs [15, 28].

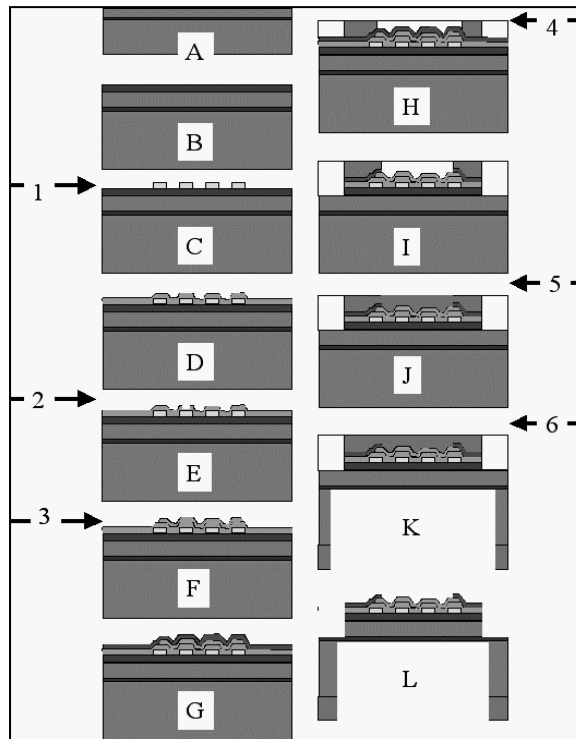


Figure 5 Illustration of process flow. For explanation see text.

As a first step, 1µm of silicon nitride is deposited on the SOI wafer (fig.5.B); lithographic patterning of a titanium/gold traces (25nm/500nm; fig.5.C) and subsequent localized nitride (700nm; fig.5 D and E) covering is performed using photo mask no.1 and 2 (arrows 1/2 in fig.5). Mask 3 is used for patterning the actual electrode sites from a chromium/iridium layer (20nm/300nm; fig.5 F). This layer is covered by another 1µm nitride deposition (1µm; fig.5 G) and another lithographical patterned layer of photo resist (mask no.4; fig.5 H). The isolating nitride layer is then removed by an appropriate dry etch (fig.5 I), which essentially leaves the iridium electrodes in a working condition. They are then once more covered with patterned photo resist (mask no. 5; fig.5 J). Utilizing back-side lithography with mask 6 prepares the wafer to un-isotropic DRI etching, forming deep trenches into the wafer's backside all the way "up" to the buried insulator layer (fig.5 K). Front-side etching and photo resist stripping removes all unwanted bulk silicon and leaves the probes suspended on the thin insulator (fig.5 L).

The SOI wafer not only provides a convenient etch stop, but enables us to hold the whole wafer in one piece for further batch processing. Details on the process will be published elsewhere.

2.3 Probe design for particular requests

As can already be seen in fig.4, a particular neurophysiological question always relates to a more or less well defined area within a brain. Therefore, the experimenter needs to influence the MEMS design before the process is performed.

The following describes the experiments and the probes designs resulting from that:

2.3.1 Cerebellar recordings

Our experimental objective is to test and use the probes for recording multiple single unit activity in the rat cerebellum. Cerebellar Golgi cells and granule cells form an oscillatory network which leads to synchronized firing of Golgi cells along the parallel fiber axis [29-31]. The probes need to be optimized to record activity in the three layers of cerebellar cortex and will be implanted in rows along the transverse axis (parallel fiber axis). Probes are intended to allow us to record from at least 3-5 Purkinje cells per applicable site along a parallel fiber beam at the same time, while also recording activity in the granular layer.

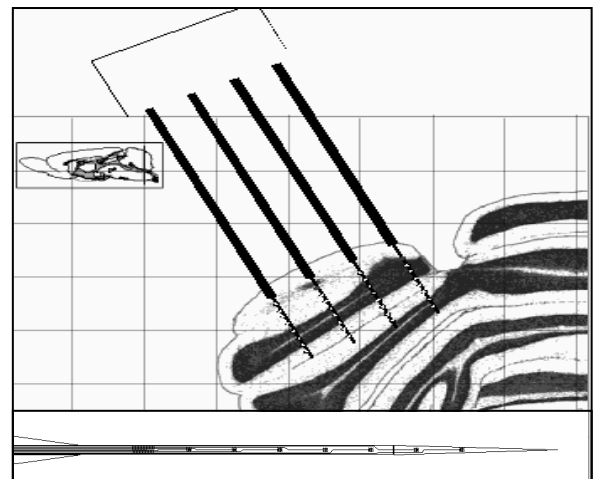


Figure 6 First version of probe design for cerebellar recordings: Schematics of a probe in its designated recording area in the cerebellum with a 1mm stereotaxic grid [32]. The lower insert shows the first 1.2mm of a single prong.

The simple spike activity of Purkinje cells will be related to the synchronized firing of Golgi cells during spontaneous and stimulus-evoked activity. Our primary cerebellar design (**fig.6**) consists thereof of

4 prongs of 5mm length, carrying 8 electrodes each. The prongs are 400 μ m center to center apart from each other. 10 μ m \times 10 μ m iridium electrodes are distributed in one line on the business end of the prongs with 100 μ m center-to-center distance. The upper most electrode is of 1000 μ m² area and will be used for electric lesioning by a DC-current [4]. The prongs have an opening taper of 4°, which makes a distance of 210 μ m from their very tip to the first electrode.

2.3.2 Cortical recordings

We intend furthermore to record extracellular field responses during acute experiments performed on the isolated guinea pig brain preparation maintained *in vitro* by arterial perfusion [33-35].

Cortical oscillations of *gamma* activity, caused by muscarinic cholinergic activation will be recorded. The study will be conducted with 32 electrodes at different cortical sites (entorhinal, perirhinal cortices, hippocampus) on both hemispheres. Patterns of cortical activation, propagation and correlation of fast gamma activity in the limbic cortex will be investigated. Recordings will therefor require horizontally widely spaced prongs with vertical less densely arranged sites than the cerebellar probe.

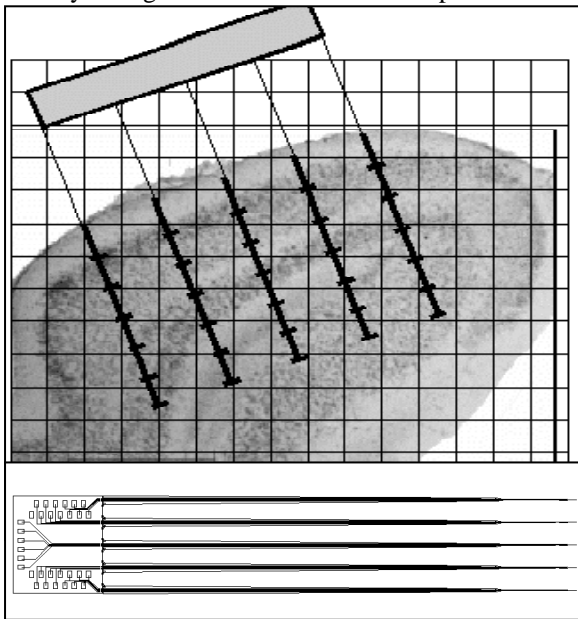


Figure 7 Schematics of a cortical probe in another cross section of a guinea pig's brain. Grid size: 250 μ m. The lower inset shows an overview over the whole probe: To the left is the bond pads carrying base plate visible.

Center-to-center distance of 5 prongs is 500 μ m with 6 electrodes spaced 250 μ m on each. Electrode arrays do not need to adapt to the slightly curved surface of the

cortex (**fig.7**) and prong length to the full wafer thickness base plate is with 10mm quite long.

2.3.3. Peripheral recordings

This first phase will consist of experiments conducted on the anaesthetized rabbit preparation to record and extract information from extracellular potentials intercepted from active peripheral nerves [36, 37]. The probe for this task carries a similar electrode array as the cerebellar probe does, except a 500 μ m prong-to-prong distance. Their length becomes with 15mm unusually long. In order to support this length especially during insertion into the tough outer layers of the nerve fascicle, the shape of each prong approaches a long triangle, with the wider (200 μ m) end at the base plate.

2.3.4 Dice overview

Above mentioned experiments are just an excerpt of our whole range and **fig.8** gives an overview over one current stepper unit with 8 different silicon probe designs, each carrying 32 recordings sites. Table 1 summarizes the features of the single probes as well. All probes share a common, rectangular base plate design with 32 bond pads, allowing at that stage of the project to contact 32 passive recording channels. "Overall length" refers to the distance from the very tip to the base plate. This is an measure for the width of the prong as well, since it the overall triangular shape of small tapered prong ends there in a width of 200 μ m. "Thin length" refers to the area of minimal prong width within the overall length.

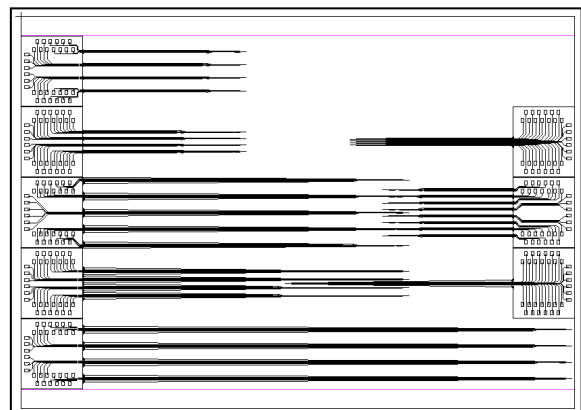


Figure 8 View over the whole stepper-unit with 8 different electrode designs.

Table 1: Design specification for above silicon probes

Ide nt. No	Prong s x Sites	Site spacin g /μm	Prong spacin g /μm	Overall length /μm	Thin length /μm
M1	1 x 32	50	-	7000	1860
M2	5 x 6	250	500	10000	1700
E1	4 x 8	100	400	5000	1200
E2	8 x 4	\approx 200	200	4000	1200
E3	4 x 8	200	200	5000	2000
K1	4 x 8	100	500	15000	1200
U1	4 x 8	100	250	10000	4000
U2	4 x 8	50	60	5000	1000

3 Conclusions

Even though we present here only preliminary results, we are confident to increase the channel count of our silicon probes to unprecedented 128 and are able to provide the neuroscience community with an easy-to-use, versatile and powerful new recording tool.

4 Literature

1. **Hodgkin, A.L. and H.J. Huxley**, *Nature*, 1939. 144: p. 710-711.
2. **Hodgkin, A.L. and A.F. Huxley**, *Journal of physiology*, 1952. 117: p. 500 - 544.
3. **Rieke, F., et al.**, eds. *Spikes - Exploring the Neural Code*. Computational Neuroscience, ed. T.J. Sejnowski and T.A. Poggio. 1998, MIT Press: Cambridge, MA. 395.
4. **Windhorst, U. and H. Johansson**, *Modern Techniques in Neuroscience Research*. 1 ed. 1999, Berlin: Springer.
5. **Kandel, E.R., J.H. Schwartz, and T.M. Jessel**, *Principles of neural science*. 3rd ed. 1991, London: Prentice-Hall.
6. **Williams, J., R. Rennaker, and D. Kipke**, **BRAIN RESEARCH PROTOCOLS**, 1999. 4(3): p. 303-313.
7. **Nicholls, J.G., A.R. Martin, and B.G. Wallace**, *From Neuron to Brain*. 3rd ed. 1992, Sunderland, MA: Sinauer Assoc., Inc. 807.
8. **Gray, C., et al.**, **JOURNAL OF NEUROSCIENCE METHODS**, 1995. 63(1-2): p. 43-54.
9. **Wise, K. and et al.**, **IEEE Trans. Biomed. Eng.**, 1970. BME-17(3): p. 238-247.
10. **Najafi, K. and K.D. Wise**, **IEEE J. Solid-State Circ.**, 1986. 21: p. 1035-1044.
11. **NAJAFI, K., K. WISE, and T. MOCHIZUKI**, **IEEE TRANSACTIONS ON ELECTRON DEVICES**, 1985. 32(7): p. 1206-1211.
12. **Buzsáki, G., et al.**, *Science*, 1992. 256: p. 1025-1027.

13. **Drake, K.L., et al.**, **IEEE Trans. Biomed. Eng.**, 1988. BME-35: p. 719-732.
14. **BUZSAKI, G., et al.**, **JOURNAL OF NEUROSCIENCE METHODS**, 1989. 28(3): p. 209-217.
15. **Kewley, D.T., et al.**, **Sensors and Actuators A**, 1997. 58: p. 27-35.
16. **Hofmann, U.G., et al.**, **Europ. J. Neurosci.**, 1998. 10(Supp. 10): p. 431.
17. **Weber, B., et al.** in *CNS*2000*. 2000. Brugge, Belgium: Elsevier.
18. **Bragin, A., et al.**, **J. Neurosci. Meth.**, 2000. 98(1): p. 77-82.
19. **Nicolelis, M.A.L., et al.**, *Nature neuroscience*, 1998. 1(7): p. 621-630.
20. **Hofmann, U.G., D.T. Kewley, and J.M. Bower**, submitted to *J. Neurosci. Meth.*, 2000.
21. **HETKE, J., K. NAJAFI, and K. WISE**, **SENSORS AND ACTUATORS A-PHYSICAL**, 1990. 23(1-3): p. 999-1002.
22. **Wise, K.D. and K. Najafi**, *Science*, 1991. 254: p. 1335 - 1342.
23. **Bai, Q., K.D. Wise, and D.J. Anderson**, **IEEE Trans Biomed Eng.**, 2000. 47(3): p. 281-289.
24. **Porada, I., et al.**, **JOURNAL OF NEUROSCIENCE METHODS**, 2000. 95(1): p. 13-28.
25. **Baumeister, T., E.A. Avallone, and T. Baumeister III**, *Marks' Standard Handbook for Mechanical Engineers*. 8th ed. 1978, New York: McGraw-Hill Book Company.
26. **Najafi, K. and J. Hetke**, **IEEE TRANSACTIONS ON BIOMEDICAL ENGINEERING**, 1990. 37(5): p. 474-481.
27. **Edell, D.J., et al.**, **IEEE Trans Biomed Eng.**, 1992. 39(6): p. 635-643.
28. **Kovacs, G.T.A.**, *Micromachined Transducers Sourcebook*. McGraw-Hill Series in Electrical and Computer Engineering, ed. S.W. Director. 1998, Boston: WCB/MacGraw-Hill. 911.
29. **Vos, B.P., et al.**, *J. neurosci.*, 1999. 19(RC 6): p. 1-5.
30. **Maex, R. and E. De Schutter, J.** **Neurophys.**, 1998. 80: p. 2521-2537.
31. **Vos, B.P., A. Volny-Luraghi, and E. De Schutter**, **Eur. J. Neurosci.**, 1999. 11: p. 2621-2634.
32. **Swanson, L.W.**, *Brain Maps: Structure of the Rat Brain*. 1 ed. 1992, Amsterdam: Elsevier. 240.
33. **Biella, G., F. Panzica, and M. de Curtis**, **Eur. J. Neurosci**, 1996. 8: p. 1350-1357.
34. **de Curtis, M., et al.**, *J. Neurophysiol.*, 1994. 71: p. 2463-2476.
35. **de Curtis, M., et al.**, **Brain Res. Prot.**, 1998. 3: p. 221-228.
36. **Yoshida, K., K. Jovanovic, and R.B. Stein, J.** **Neurosci. Meth.**, 2000. 96: p. 47-55.
37. **Yoshida, K. and R.B. Stein**, **IEEE Trans. Biomed. Eng.**, 1999. 46(2): p. 226-234.